Superthreshold Behavior of Ultrasound-Induced Lung Hemorrhage in Adult Rats

Role of Pulse Repetition Frequency and Exposure Duration Revisited

William D. O'Brien, Jr, PhD, Douglas G. Simpson, PhD, Leon A. Frizzell, PhD, James F. Zachary, DVM, PhD

Objective. The purpose of this study was to augment and reevaluate the ultrasound-induced lung hemorrhage findings of a previous 5 × 3 factorial design study (Ultrasound Med Biol 2001; 27:267–277) that evaluated the role of pulse repetition frequency (PRF: 25, 50, 100, 250, and 500 Hz) and exposure duration (ED; 5, 10, and 20 s) on ultrasound-induced lung hemorrhage at an in situ (at the pleural surface) peak rarefactional pressure [$p_{r(in\ situ)}$] of 12.3 MPa; only PRF was found to be significant. However, saturation (response plateau) due to the high $p_{r(in\ situ)}$ might have skewed the results. In this follow-up 3 × 3 factorial design study, a wider range of PRFs and EDs were used at a lower $p_{r(in\ situ)}$. ***Methods.*** Sprague Dawley rats (n = 198) were divided into 18 ultrasonically exposed groups (10 rats per group) and 6 sham groups (3 per group). The 3 × 3 factorial design study (PRF: 17, 170, and 1700 Hz; ED: 5, 31.6, and 200 s) was conducted at 2 frequencies (2.8 and 5.6 MHz). The $p_{r(in\ situ)}$ was 6.1 MPa. Logistic regression analysis evaluated lesion occurrence, and Gaussian tobit analysis evaluated lesion depth and surface area. ***Results.*** Frequency did not have a significant effect, so the analysis combined results for the 2 frequencies. For lesion occurrence and sizes, the main effects for PRF and ED were not significant. The interaction term was highly significant, indicating a strong dependence of lesion occurrence and size on the total number of pulses (PRF × ED). ***Conclusions.*** The results of both studies are consistent with the hypothesis that the total number of pulses is an important factor in the genesis of ultrasound-induced lung hemorrhage. ***Key words:*** exposure duration; lung hemorrhage; pulsed ultrasound; pulse repetition frequency; rat lung; ultrasound bioeffects.

Abbreviations
ED, exposure duration; MI, mechanical index; p_c, peak compressional pressure; PRF, pulse repetition frequency; p_r, peak rarefactional pressure

Received August 25, 2004, from the Bioacoustics Research Laboratory, Department of Electrical and Computer Engineering, University of Illinois, Urbana, Illinois USA (W.D.O., L.A.F.); Department of Statistics, University of Illinois, Champaign, Illinois USA (D.G.S.); and Department of Veterinary Pathobiology (J.F.Z.), University of Illinois, Urbana, Illinois USA. Revision requested September 13, 2004. Revised manuscript accepted for publication November 5, 2004.

We thank our valued colleagues R. Bashyal, J. Blue, Jr, J. Christoff, K. Clements, O. Coffield, T. Fong, R. Miller, K. Norrell, P. Patel, S. Sakai, A. Tevar, R. Towa, E. Wort, Y. Yang, and B. Zierfuss for technical contributions. This work was supported by National Institutes of Health grant EB02641 (formerly HL58218) awarded to W.D.O. and J.F.Z. and by National Science Foundation grant DMS-0073044 awarded to D.G.S.

Address correspondence and reprint requests to William D. O'Brien, Jr, PhD, Bioacoustics Research Laboratory, Department of Electrical and Computer Engineering, University of Illinois, 405 N Mathews, Urbana, IL 61801 USA.

E-mail: wdo@uiuc.edu

A previous 5 × 3 factorial design study evaluated the role of pulse repetition frequency (PRF: 25, 50, 100, 250, and 500 Hz) and exposure duration (ED: 5, 10, and 20 s) on ultrasound-induced lung hemorrhage and the PRF × ED interaction.[1] In that study, the lesion characteristics produced in mice and rats at 2.8 MHz were similar to those described in previous studies,[1–19] suggesting a common pathogenesis for the initiation and propagation of the lesions at the gross and microscopic levels. Furthermore, the proportion of lesions in both species was related statistically to PRF and ED, with the exception that PRF in rats was not quite sig-

nificant; the PRF × ED interaction (number of pulses) for lesion production was not significant for either species. However, as PRF, ED, or both increased, the percentage of animals with lesions approached 100% for both species, suggesting saturation of ultrasound-induced lesion production and thus calling into question the study's conclusions on PRF and ED dependencies. It was even suggested in the previous study that a clearer picture of the dependencies on PRF, ED, and PRF × ED might be expected if a lower in situ (at the pleural surface) peak rarefactional pressure [$p_{r(\text{in situ})}$] value were to be investigated.

The $p_{r(\text{in situ})}$ value selected for the previous study was designed to be large enough to ensure a sufficient number of lesions to test the dependency of lesion formation and size on PRF (25, 50, 100, 250, and 500 Hz) and ED (5, 10, and 20 s); the number of pulses ranged between 125 and 10,000. The $p_{r(\text{in situ})}$ value of 12.3 MPa was based on our previous findings[15] in which the percentage of mice and rats with lesions was 80% at an ultrasonic frequency of 2.8 MHz and a $p_{r(\text{in situ})}$ value of about 11 MPa (the PRF was 1 kHz, and the ED was 10 s, which yielded 10,000 pulses per exposure). Therefore, it was our view that we needed to use a relatively high $p_{r(\text{in situ})}$ value because the exposure conditions (based on total number of pulses) were equal to or less than 10,000 pulses per exposure. We recognized that a $p_{r(\text{in situ})}$ of 12.3 MPa was considerably greater than that allowed under current regulations.[20] At a $p_{r(\text{in situ})}$ of 12.3 MPa, the mechanical indices (MIs)[21] for mice and rats were, respectively, 6.3 and 7.1, whereas the US Food and Drug Administration regulatory limit is 1.9 for diagnostic ultrasound equipment.

Thus, a new PRF × ED factorial design study is reported herein that uses a lower $p_{r(\text{in situ})}$ value of 6.1 MPa to not saturate lesion production. Furthermore, because our previous exposure-effect ultrasound-induced lung hemorrhage studies have not shown differences between mice and rats,[1,15] only rats were used. In addition, the ranges of PRF and ED values have been increased [PRF: 17, 170, and 1700 Hz; ED, 5, 31.6, and 200 s (parametric in the log domain)] to include typical clinical exposure values. Finally, 2 frequencies are evaluated (2.8 and 5.6 MHz). The effect of these 2 frequencies for the same $p_{r(\text{in situ})}$ value (6.1 MPa) on the MI yields an MI of 3.1 at 2.8 MHz and an MI of 1.5 at 5.6 MHz.

Materials and Methods

Exposimetry

The exposimetry and calibration procedures have been described previously in considerable detail.[15] Two focused, 19-mm-diameter, lithium niobate ultrasonic transducers (Valpey Fisher, Hopkinton, MA) were used. Water-based (degassed water, 22 ± 0.5°C) pulse-echo ultrasonic field distribution measurements were performed (Table 1) according to established procedures.[15,22]

An automated procedure routinely calibrated the ultrasound fields[15] and was based on established standards.[21,23] Briefly, the source transducer was mounted in a water tank (degassed water, 22 ± 0.5°C), and its drive voltage was supplied by a RAM5000 ultrasound system (Ritec, Inc, Warwick, RI). A calibrated polyvinylidene difluoride membrane hydrophone (model Y-34-6543; Marconi, Chelmsford, England), mounted to a computer-controlled micropositioning system (Daedal, Inc, Harrisburg, PA), scanned the ultrasound field along the determined beam axis. The hydrophone's signal was digitized with an oscilloscope (500 MS/s; model 9354TM; LeCroy, Chestnut Ridge, NY) and transferred to the same computer (Dell Pentium II; Dell Corporation, Round Rock, TX) that controlled the positioning system. The radio frequency data were transferred to a workstation and analyzed with MATLAB (The MathWorks, Natick, MA).

The radio frequency hydrophone waveforms were processed to yield the water-based $p_{r(\text{in vitro})}$ and the in vitro peak compressional pressure [$p_{c(\text{in vitro})}$] (Table 2). The MI was also determined.[21] The purpose for providing the MI is because it is a regulated quantity[20] of diagnostic ultrasound systems, and its magnitude is available to system operators.

A total of 18 independent calibrations of the 2.8-MHz transducer and 17 independent calibrations of the 5.6-MHz transducer were conducted during the 3-month period of the experiments. At the exposure levels used in this study, the relative SDs (SD × 100/mean) were 11% for $p_{r(\text{in vitro})}$ and 12% for $p_{c(\text{in vitro})}$ for the 2.8-MHz transducer and 14% for $p_{r(\text{in vitro})}$ and 16% for $p_{c(\text{in vitro})}$ for the 5.6-MHz transducer. The pulse durations were also measured[23] at every calibration for both transducers: 1.3 μs (2.8 MHz) and 1.1 μs (5.6 MHz).

The $p_{r(in\ situ)}$ and $p_{c(in\ situ)}$ (at the pleural surface) were estimated by derating the maximum water-based $p_{r(in\ vitro)}$ and $p_{c(in\ vitro)}$ values by the mean insertion loss of the rat's intercostal tissue of 2.8 dB/cm at 2.8 MHz and 5.9 dB/cm at 5.6 MHz[24,25] and its chest wall thickness of 3.6 ± 0.3 mm (mean ± SD).

The experimental protocol required the same $p_{r(in\ situ)}$ for all exposed animals. Rat chest wall insertion losses and thicknesses were used from previous experiments[1,15,24,25] to estimate the $p_{r(in\ vitro)}$ values that would correspond to the same $p_{r(in\ situ)}$ value. The actual $p_{r(in\ situ)}$ values obtained in this study were determined from the measured chest wall thicknesses of the animals used herein, and the chest wall insertion losses were those previously determined.[24,25] Thus, for both frequencies, $p_{r(in\ situ)}$ was 6.1 MPa, the quantity used for the study protocol.

Animals

The experimental protocol was approved by the campus Laboratory Animal Care Advisory Committee and satisfied all campus and National Institutes of Health rules for the humane use of laboratory animals. Rats were housed in an animal facility approved by the Association for Assessment and Accreditation of Laboratory Animal Care, placed in groups of 3 or 4 in polycarbonate cages with Beta Chip bedding (NEPCO, Warrensburg, NY) and wire bar lids, and provided food and water ad libitum.

A total of 198 10- to 11-week-old 241 ± 14-g (mean ± SD) female Sprague Dawley rats (Harlan, Indianapolis, IN) were divided into 18 ultrasonically exposed groups (10 rats per group) and 6 sham groups (3 rats per group for each of the 6 ED frequency groups). Each frequency included 9 ultrasonically exposed groups and 3 sham groups; there were no lesions in the 18 sham-exposed rats. The experiment was a 3 × 3 factorial design with 3 PRF groups and 3 ED groups. Rats were randomly divided among the 12 different groups for each frequency. The $p_{r(in\ situ)}$ value was the same for all ultrasonically exposed groups. The individuals involved in animal handling, exposure, and lesion scoring were blinded to the exposure condition. The exposure conditions for each animal were revealed only after the final results were tabulated.

Rats were weighed and then anesthetized with ketamine hydrochloride (87.0 mg/kg) and xylazine (13.0 mg/kg) administered intraperitoneally. For each rat, the skin of the left thorax was exposed by removing the hair with an electric clipper, followed by a depilatory agent (Nair; Carter-Wallace, Inc, New York, NY) to maximize sound transmission. A black dot was placed on the skin over the ribs at approximately the sixth to ninth rib to guide the positioning of the ultrasonic beam. The anesthetized rat was placed in a specially designed holder. The ultrasonic transducer was attached to the holder. A removable pointer, attached to the transducer, was used to position the ultrasonic beam perpendicular to the skin at the position of the black dot with the beam's focal region approximately at the lung surface.[1,15]

The holder with the animal and mounted transducer was placed in degassed, temperature-controlled (30 ± 0.5°C) water. The low-power pulse-echo capability of the exposure system (RAM5000) displayed on an oscilloscope was used to adjust the axial center of the focal region to within 1 mm of the lung surface. It was during this part of the experimental procedure that the 13-Ω in-line attenuator was placed between the RAM5000 and transducer to obtain sham exposure values (Table 2). Also, the PRF was 10 Hz during this alignment procedure. All ultrasonically exposed animals received the

Table 1. Water-Based Pulse-Echo Ultrasonic Field Distribution Results for the Two 19-mm-Diameter Lithium Niobate Ultrasonic Transducers

	Center Frequency, MHz	
Parameter	**2.8**	**5.6**
Fractional bandwidth, %	12	13
Focal length, mm	19	38
–6-dB focal beam width, μm	470	510
–6-dB depth of focus, mm	2.7	6.9

Table 2. In Vitro (in Water) and In Situ (at the Pleural Surface) Peak Rarefactional and Peak Compressional Pressures

	2.8 MHz		5.6 MHz	
Parameter	**Sham**	**Exposed**	**Sham**	**Exposed**
$p_{r(in\ vitro)}$, MPa	0.30	6.8	0.65	7.9
$p_{c(in\ vitro)}$, MPa	0.36	7.8	0.64	17
$p_{r(in\ situ)}$, MPa	0.27	6.1	0.51	6.1
$p_{c(in\ situ)}$, MPa	0.32	7.0	0.50	13
MI	0.15	3.1	0.12	1.5

All rats were exposed to pulsed ultrasound. The sham exposure conditions used a PRF of 10 Hz. The MI is provided because this is a regulated quantity of diagnostic ultrasound equipment.[20]

same $p_{r(in\ situ)}$ of 6.1 MPa. The PRF (17, 170, and 1700 Hz) and ED (5, 31.6, and 200 s) were randomly assigned to each animal. During the exposure, each rat was observed for changes in its breathing pattern and respiratory rate. After exposure, the rat was removed from the water and holder and then euthanized under anesthesia by cervical dislocation.

The thorax was opened, and the thickness of each left thoracic wall (skin, rib cage, and parietal pleura) at the point of exposure was measured with a digital micrometer (accuracy, 10 μm; Mitutoyo Corp, Kawasaki, Kanagawa, Japan). These chest wall measurements were used for later calculation of the in situ ultrasonic pressures at the visceral pleural surface. The lungs were removed from each rat, and the left lung lobe was scored for the presence or absence of hemorrhage. The left lung was fixed by immersion in 10% neutral-buffered formalin until the tissue was adequately fixed.[26] Although satisfactory fixation can be obtained in 24 hours, the fixation period was greater than 1 week. After fixation, the elliptical dimensions of each lung lesion at the visceral pleural surface were measured with a digital micrometer in which "a" was the semimajor axis and "b" was the semiminor axis. The surface area (πab) of the lesion was calculated for each animal. The lesion was then bisected, and the depth ("d") of the lesion within the pulmonary parenchyma was also measured. Each half of the bisected lesion was embedded in paraffin, sectioned at 5 μm, stained with hematoxylin and eosin, and evaluated microscopically.

Statistics

The effects of PRF (17, 170, and 1700 Hz) and ED (5, 31.6, and 200 s) were evaluated in a 3×3 factorial design. Rat lungs were exposed to ultrasound at a $p_{r(in\ situ)}$ of 6.1 MPa. The primary end points were lesion occurrence and depth in and surface area of exposed lungs. The design was the same at frequencies of 2.8 and 5.6 MHz. Ten animals were exposed at each combination of PRF, ED, and frequency. Logistic regression analysis and Gaussian tobit analysis were used to assess the significance of PRF and ED on the occurrence and size of lesions as previously described.[1,15,17,18] All statistical calculations were performed using the R statistical software package,[27] which is distributed for free.[28]

The logistic regression models were estimated from occurrence data using the R function "glm," which calculated maximum likelihood estimates, SEs, and model statistics as described.[29] Let n_{ij} denote the number of animals with ED_i and PRF_i, and let Y_{ij} denote the number of animals exhibiting lesions in this group. Furthermore, let π_{ij} denote the probability of a lesion for ED_i and PRF_i. Then, according to the model, Y_{ij} is binomially distributed with trials and event probability π_{ij}. For a given frequency, the full interaction model has the form

$$(1) \quad \log\left(\frac{\pi_{ij}}{1-\pi_{ij}}\right) = \alpha + \beta_i^{PRF} + \beta_j^{ED} + \gamma_{ij}^{PRF\times ED},$$

where α is the baseline value; β_i^{PRF} is the main effect for PRF; β_j^{ED} is the main effect for ED; $\gamma_{ij}^{PRF\times ED}$ is the interaction parameter, and (i = 1, j = 1) is the baseline cell in the design so that

$$\beta_1^{PRF} = \beta_1^{ED} = \gamma_{1j}^{PRF\times ED} = \gamma_{i1}^{PRF\times ED} = 0.$$

Each of the coefficients represents an increment in the log-odds of a lesion compared with the reference exposure of $PRF = PRF_1 = 17$ Hz and $ED = ED_1 = 5$ s. Initially, the model (Equation 1) was fit for each ultrasound frequency, and then a likelihood ratio test was performed to determine whether both frequencies could be combined.

Trend models were also considered, in which the log-odds depend linearly on numerical values of PRF (in kHz), ED (in 100 s) and their product,

$$(2) \quad \log\left(\frac{\pi_{ij}}{1-\pi_{ij}}\right) = \alpha + \beta_1 PRF_i + \beta_2 ED_j + \gamma_{12} PRF_i \times ED_j,$$

where α is the baseline value; β_1 is the PRF coefficient; β_2 is the ED coefficient; and γ_{12} is the interaction coefficient. A likelihood ratio test between the trend model (Equation 2) and the full model (Equation 1) provided an assessment of the fit of the trend model.[30] χ^2 tests of the coefficients in the model were used to determine statistical significance of PRF, ED, and the interaction.

Data on lesion depth and root surface area ($\sqrt{\text{surface area}}$) were analyzed by Gaussian tobit regression,[31] as previously described.[1,15,17,18] The computations were performed using the "survreg" function in R.[32] Tobit regression is a model for positive valued responses with a threshold at 0. If the lung shows a lesion, then the response is the measured depth (or root surface area) of the lesion. If no lesion is present, then the depth is 0. Let Z_{ijk} denote the depth (or root surface area) for the kth animal with $PRF = PRF_i$ and

ED = ED_j. The tobit regression model entails that Z_{ijk} has a normal distribution truncated below at 0. Let μ_{ij} denote the mean of the untruncated normal distribution, and let σ^2 denote its variance. If μ_{ij} is positive, then it is also the median lesion size (depth or root surface area), whereas if μ_{ij} is negative, then the median lesion size is 0. The full interaction model for the factorial design specifies that

$$\mu_{ij} = \alpha + \beta_i^{PRF} + \beta_j^{ED} + \gamma_{ij}^{PRF \times ED}, \quad (3)$$

where the coefficients satisfy the same constraints as in the logistic regression model above. The simplified trend model has the form

$$\mu_{ij} = \alpha + \beta_1 PRF_i + \beta_2 ED_j + \gamma_{12} PRF_i \times ED_j, \quad (4)$$

where the coefficients and variables are defined in the same way as in the logistic regression model above. The tobit models were fit by the method of maximum likelihood using the R "survreg" function, and median lesion depth and surface area were computed from the model for each exposure level.

Results

As PRF, ED, or both increased for both frequencies, the percentage of rats with lesions did not appear to increase until higher PRFs and EDs were used (Figure 1).

The logistic regression models corresponding to Equations 1 and 2 were fit to the lesion occurrence data. Frequency did not have a significant effect in the model, so the analysis combined results for both frequencies. The likelihood ratio test of the trend model (Equation 2) versus the full model (Equation 1) indicated that the trend model was adequate for the data ($P > .2$). Furthermore, the main effects for PRF and ED in the trend model were not significant at $P = .05$, and a simplified trend model depending only on the product term PRF × ED was found to be sufficient. Table 3 provides a summary of the final logistic regression trend model including coefficient estimates, SEs, χ^2 values, and P values. The P values are the observed significance levels of tests that the respective coefficients equal 0. The product interaction term, PRF × ED, is highly significant in the model, indicating a strong dependence of lesion occurrence on the total number of pulses (PRF × ED). The observed proportions and estimated probabilities of lesions are given in Table 4, which shows how the PRF effect becomes more pronounced as ED increases from 5 to 200 s. Figure 2A shows the observed proportions of lesions and estimated probabilities as functions of PRF × ED.

The analogous tobit models were fit to the data on lesion depth and root surface area (Figure 1). The final fitted models are summarized in Tables 5 and 6. It was found that depth and surface area of lesions depend significantly on the product of PRF and ED, that is, PRF × ED. Compared with logistic regression of incidence, these models have an extra parameter (σ) to model the variation in the size of the lesion about the predicted size. As in the logistic regression model, the interaction between PRF and ED is highly significant, whereas the main effects are not significant at $P = .05$. The PRF trend is stronger for longer EDs, and the median lesion size exhibits a strong dependence on the total number of pulses. Tables 7 and 8 show sample 75th percentiles and 75th percentiles computed from the tobit regression model for each combination of PRF and ED. It should be observed that each sample 75th percentile is based on 20 observations, and they display considerable variability. An observed value of 0 means that at least 75% of the lungs had no lesions at all. The sample and model-based percentiles are plotted in Figure 2, B and C, to show the dependence on the number of ultrasound pulses.

Discussion

The primary result of the analysis is the statistically significant positive dependence of lesion occurrence and lesion size on the interaction between PRF and ED, in other words, on the total number of ultrasound pulses, and the main effects for PRF and ED were not significant for lesion occurrence or lesion size. Previously, however, the PRF × ED interaction was not significantly different in rats for lesion occurrence and lesion size, whereas the main effects for PRF and ED showed mixed findings: lesion occurrence was dependent on ED but not on PRF; lesion depth was dependent on PRF but not on ED; and lesion area was not dependent on either PRF or ED.[1] It is plausible that both the limited PRF and ED range and the saturation (nonlinearity) due to the higher $p_{r(in\ situ)}$ of 12.3 MPa of the previous study [compared with the $p_{r(in\ situ)}$ of 6.1 MPa for

this study] reduced the power to detect PRF and ED effects, either as main effects or as an interaction. In this study, a strong effect was observed only at the highest PRF, and this would have been in the saturation zone of the previous experiment with its higher $p_{r(in\ situ)}$ level.

Although the logistic linear model and tobit linear models fit reasonably well herein, according to goodness of fit tests, the data suggest possible saturation at the highest level of PRF × ED with PRF = 1.7 kHz and ED = 200 s. The observed proportion of lesions and percentiles of size are nearly the same as for PRF = 1.7 kHz and ED= 31.6 s. The phenomenon is evident for the highest 2 exposure levels (Figure 2). Thus, whereas a high PRF appears necessary to significantly increase the occurrence and growth of lesions, only a moderate ED at this high PRF × ED level is sufficient to induce the maximal degree of hemorrhaging. Overall, the trends for lesion depth

Figure 1. Mean lesion occurrence, depth, surface area, and volume in rats as a function of PRF for the 3 EDs. Left panels are 2.8-MHz exposure, and right panels are 5.6-MHz exposure. Error bars represent SEM.

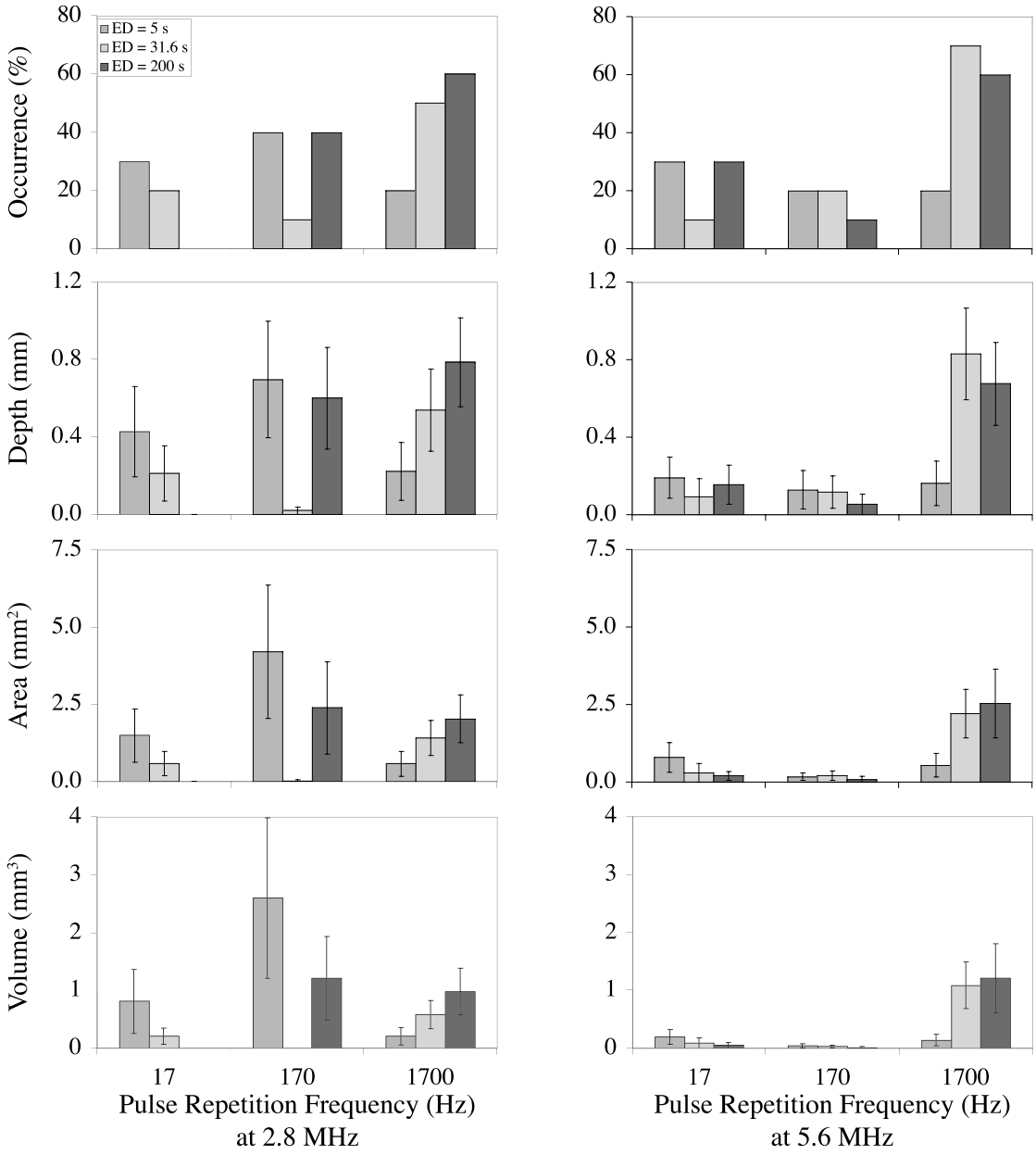

and surface area are parallel with the probability trends in the logistic regression analysis of lesion occurrence. In particular, PRF has a more pronounced effect over longer ED.

If saturation is a modifying effect, then it was much more evident in the previous study[1] than in the study reported herein. Figure 3 compares lesion occurrence and size in rats from both studies and shows that, in the previous study, which was conducted at a much higher $p_{r(in\ situ)}$ of 12.3 MPa, of 15 exposure conditions (the previous study had a 5×3 factorial design), 11 yielded a mean lesion occurrence rate of 80% or greater. However, in the study reported herein, which was conducted at a lower $p_{r(in\ situ)}$ of 6.1 MPa, of 9 exposure conditions, the highest mean lesion occurrence rate was 70%.

Another notable finding is that lesion occurrence and lesion size are not dependent on ultrasound frequency over the range of the experiment (2.8 and 5.6 MHz). Frequency independence has been a consistent finding of ultrasound-induced lung hemorrhage[1,15] and provides additional support, along with the previous findings that inertial cavitation is not responsible for ultrasound-induced lung hemorrhage,[12,19,33] that the MI should be reevaluated as an index for regulatory purposes.[20,21]

It is interesting to note that thermal lesions produced in mammalian brain tissue by single ultrasound pulse exposures (1- to 100-s pulse durations) were also essentially frequency independent over the 1- to 10-MHz frequency range.[34] This result was explained as the approximate cancellation of the effects of increasing absorption and decreasing beam width with increasing frequency; focused transducers were used, and the beam width decreased with increasing frequency. The former increased the heat generation rate, and the latter increased conduction of heat from the focal region, resulting in similar temperature rises versus frequency for these thermally produced lesions. However,

Table 3. Logistic Regression Model for Occurrence of Lesions: Active Variables Are PRF (in kHz) and ED (in 100 s)

Variable	Coefficient	SE	χ^2	*df*	*P*
Intercept	–1.129	0.189	35.6	1	<.0001
PRF × ED	0.503	0.151	11.01	1	.0009

Table 4. Observed Proportions of Lesions and Probability Estimates (in Parentheses) Based on Logistic Regression Model

Variable	PRF = 17 Hz	PRF = 170 Hz	PRF = 1700 Hz
ED = 5 s	0.30 (0.244)	0.30 (0.245)	0.20 (0.252)
ED = 31.6 s	0.15 (0.245)	0.15 (0.249)	0.60 (0.298)
ED = 200 s	0.15 (0.248)	0.25 (0.277)	0.60 (0.641)

Figure 2. A, Observed proportions of lesions and estimated (fitted) probabilities of lesions based on logistic regression model. **B**, Seventy-fifth percentile of lesion depth based on sample percentiles (observed) and model based-percentiles (fitted). **C**, Seventy-fifth percentile of the square root of the lesion surface area based on sample percentiles (observed) and model-based percentiles (fitted) as a function of the total number of ultrasound pulses (PRF in Hz, ED in s, and log displayed).

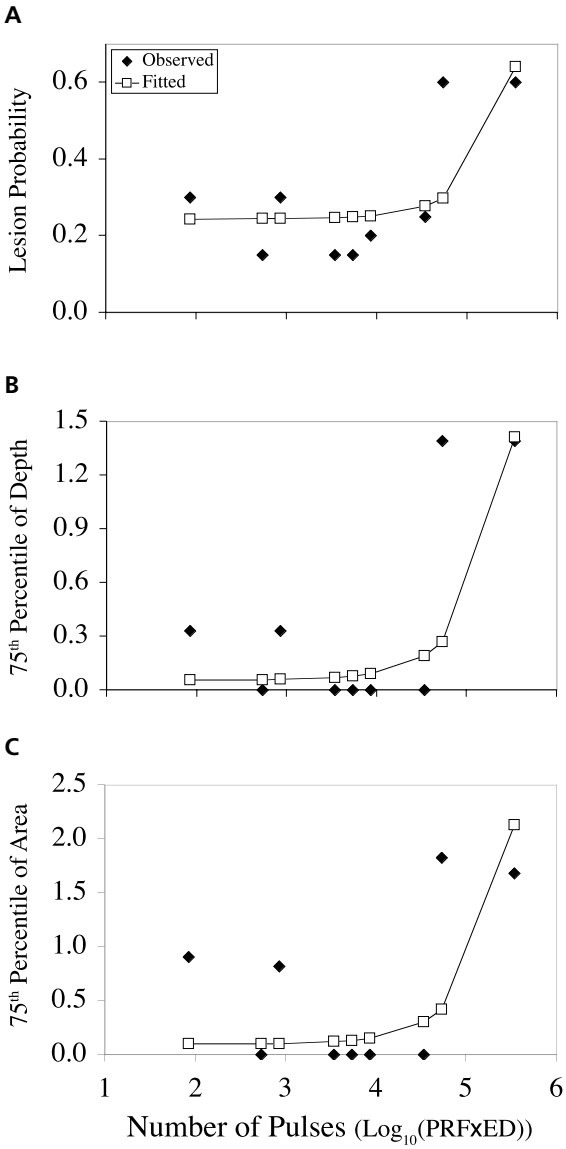

in our case, different transducers were used at the 2 frequencies with the intent of maintaining approximately the same beam width at both frequencies. Thus, the explanation of the frequency-independent brain lesions does not apply to our results for 2 reasons: the hemorrhage produced in the lung is believed to be due to a nonthermal mechanism, and the beam width in our study was maintained constant with frequency.

In comparing the results of this study with previous results, the lack of main effects for ED and PRF does not imply that these variables have no effect but, rather, that the strongest effect is the total number of pulses (ED × PRF). If either variable is held relatively constant or varied over only a narrow range, then the number of pulses will appear as an effect of the nonconstant variable: the interaction reduces to a main effect of ED if PRF is held constant and vice versa. Thus, our results are consistent with those of Child et al,[2] who showed a slightly larger proportion of mice with lesions for 100-Hz PRF compared with 10-Hz PRF (1.2 MHz, 10-µs PD and 180-s ED). Our results are also consistent with those of Raeman et al,[9] who showed a greater proportion of mice with lesions for a 180-s ED compared with a 20-s ED (2.3 MHz, 10-µs PD and 100-Hz PRF). However, when the number of pulses was held constant for 2 exposure conditions, Raeman et

Table 5. Summary of Tobit Model for Lesion Depth: Active Variables Are PRF (in kHz) and ED (in 100 s)

Variable	Coefficient	SE	χ^2	*df*	*P*
Intercept	–0.906	0.213	18.1	1	<.0001
PRF × ED	0.339	0.116	11.8	1	.0006
log(σ)	0.355	0.114	9.67	1	.0019

Table 6. Summary of Tobit Model for Square Root Lesion Surface Area: Active Variables Are PRF (in kHz) and ED (in 100 s)

Variable	Coefficient	SE	χ^2	*df*	*P*
Intercept	–1.435	0.340	17.8	1	<.0001
PRF × ED	0.596	0.185	10.4	1	.0013
log(σ)	0.822	0.114	52.1	1	.0010

Table 7. Sample 75th Percentiles and Model-Based 75th Percentiles (in Parentheses) for Lesion Depth (in mm)

Variable	PRF = 17 Hz	PRF = 170 Hz	PRF = 1700 Hz
ED = 5 s	0.33 (0.056)	0.33 (0.59)	0.00 (0.90)
ED = 31.6 s	0.00 (0.058)	0.00 (0.077)	1.39 (0.27)
ED = 200 s	0.00 (0.069)	0.00 (0.12)	1.39 (1.41)

Table 8. Sample 75th Percentiles and Model-Based 75th Percentiles (in Parentheses) for Root Lesion Surface Area (in mm^2)

Variable	PRF = 17 Hz	PRF = 170 Hz	PRF = 1700 Hz
ED = 5.0 s	0.91 (0.10)	0.82 (0.10)	0.00 (0.15)
ED = 31.6 s	0.00 (0.10)	0.00 (0.13)	1.83 (0.42)
ED = 200.0 s	0.00 (0.12)	0.00 (0.30)	1.68 (2.13)

Figure 3. Comparison of mean lesion occurrence, depth, and surface area in rats as a function of the total number of ultrasound pulses (PRF in Hz, ED in s, and log displayed) for the study reported herein and the previous study.[1] Error bars represent SEM.

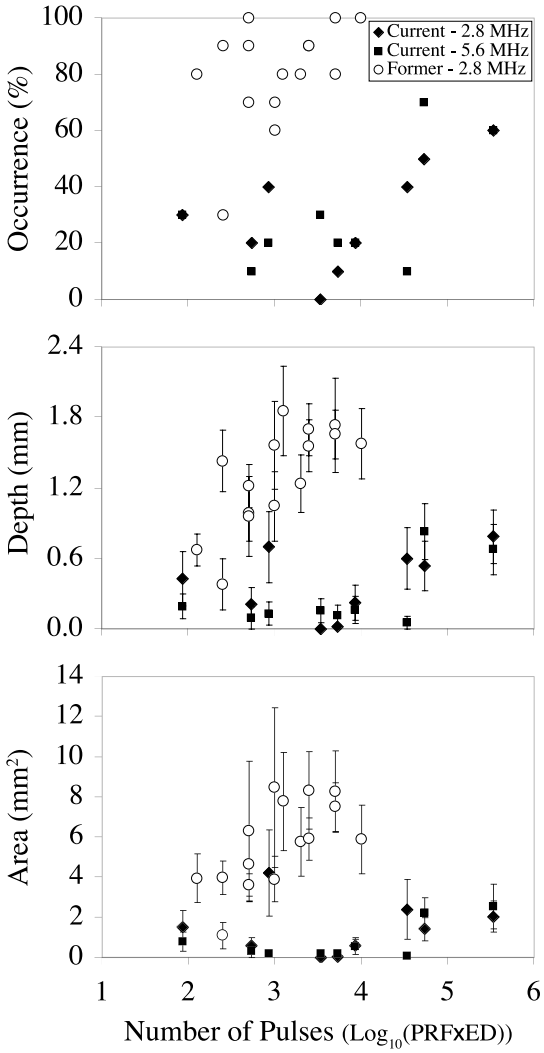

al[4] showed that the lesion volume was greater for 3-min ED than for 0.3-min ED, although the PRF was changed from 100 to 1000 Hz, a finding that is not consistent with our results.

In our previous study,[1] it was suggested that PRF and ED timing quantities should be considered within the definition of the MI, which applies to nonthermal mechanisms such as that operative in ultrasound-induced lung hemorrhage. This suggestion now needs to be expanded because, as reported herein, with wider ranges of ED and PRF, the effects of PRF and ED are synergistically expressed through their product, the total number of pulses. The previous study, which had a narrower range of PRF and saturation effects, did not detect the magnifying effect of PRF on ED reflected in the new results. These new data indicate that the MI definition may need to consider the number of pulses (product of PRF and ED) rather than the individual variables. Furthermore, because of the consistent frequency-independent ultrasound-induced lung hemorrhage findings, it is suggested that a new index for diagnostic ultrasound regulatory proposes be considered to quantify nonthermal mechanisms, at least for the lung.

References

1. O'Brien WD Jr, Frizzell LA, Schaeffer DJ, Zachary JF. Superthreshold behavior of ultrasound-induced lung hemorrhage in adult mice and rats: role of pulse repetition frequency and exposure duration. Ultrasound Med Biol 2001; 27:267–277.
2. Child SZ, Hartman CL, Schery LA, Carstensen EL. Lung damage from exposure to pulsed ultrasound. Ultrasound Med Biol 1990; 16:817–825.
3. Penney DP, Schenk EA, Maltby K, Hartman-Raeman C, Child SZ, Carstensen EL. Morphologic effects of pulsed ultrasound in the lung. Ultrasound Med Biol 1993; 19:127–135.
4. Raeman CH, Child SZ, Carstensen EL. Timing of exposures in ultrasonic hemorrhage of murine lung. Ultrasound Med Biol 1993; 19:507–512.
5. Frizzell LA, Chen E, Lee C. Effects of pulsed ultrasound on the mouse neonate: hind limb paralysis and lung hemorrhage. Ultrasound Med Biol 1994; 20:53–63.
6. Tarantal AF, Canfield DR. Ultrasound-induced lung hemorrhage in the monkey. Ultrasound Med Biol 1994; 20:65–72.
7. Zachary JF, O'Brien WD Jr. Lung lesion induced by continuous- and pulsed-wave (diagnostic) ultrasound in mice, rabbits, and pigs. Vet Pathol 1995; 32:43–45.
8. Holland CK, Deng CX, Apfel RE, Alderman JL, Fenandez LA, Taylor KJW. Direct evidence of cavitation in vivo from diagnostic ultrasound. Ultrasound Med Biol 1996; 22:917–925.
9. Raeman CH, Child SZ, Dalecki D, Cox C, Carstensen EL. Exposure-time dependence of the threshold for ultrasonically induced murine lung hemorrhage. Ultrasound Med Biol 1996; 22:139–141.
10. Dalecki D, Child SZ, Raeman CH, et al. Age dependence of ultrasonically induced lung hemorrhage in mice. Ultrasound Med Biol 1997; 23:767–776.
11. Dalecki D, Child SZ, Raeman CH, Cox C, Carstensen EL. Ultrasonically induced lung hemorrhage in young swine. Ultrasound Med Biol 1997; 23: 777–781.
12. O'Brien WD Jr, Frizzell LA, Weigel RM, Zachary JF. Ultrasound-induced lung hemorrhage is not caused by inertial cavitation. J Acoust Soc Am 2000; 108: 1290–1297.
13. O'Brien WD Jr, Simpson DG, Frizzell LA, Zachary JF. Superthreshold behavior and threshold estimation of ultrasound-induced lung hemorrhage in adult rats: role of beamwidth. IEEE Trans Ultrason Ferroelectr Freq Control 2001; 48:1695–1705.
14. Zachary JF, Frizzell LA, Norell KS, Blue JP Jr, Miller RJ, O'Brien WD Jr. Temporal and spatial evaluation of lesion reparative responses following superthreshold exposure of rat lung to pulsed ultrasound. Ultrasound Med Biol 2001; 27:829–839.
15. Zachary JF, Sempsrott JM, Frizzell LA, Simpson DG, O'Brien WD Jr. Superthreshold behavior and threshold estimation of ultrasound-induced lung hemorrhage in adult mice and rats. IEEE Trans Ultrason Ferroelectr Freq Control 2001; 48:581–593.
16. Frizzell LA, O'Brien WD Jr, Zachary JF. Effect of pulse polarity and energy on ultrasound-induced lung hemorrhage in adult rats. J Acoust Soc Am 2003; 113:2912–2926.
17. O'Brien WD Jr, Simpson DG, Ho MH, Miller RJ, Frizzell LA, Zachary JF. Superthreshold behavior and threshold estimation of ultrasound-induced lung hemorrhage in pigs: role of age dependency. IEEE Trans Ultrason Ferroelectr Freq Control 2003; 50:153–169.

18. O'Brien WD Jr, Simpson DG, Frizzell LA, Zachary JF. Threshold estimates and superthreshold behavior of ultrasound-induced lung hemorrhage in adult rats: role of pulse duration. Ultrasound Med Biol 2003; 29:1625–1634.

19. O'Brien WD Jr, Simpson DG, Frizzell LA, Zachary JF. Effect of contrast agent on the incidence and magnitude of ultrasound-induced lung hemorrhage in rats. Echocardiography 2004; 21:417–422.

20. US Food and Drug Administration. Information for Manufacturers Seeking Marketing Clearance of Diagnostic Ultrasound Systems and Transducers. Rockville, MD: Center for Devices and Radiological Health, US Food and Drug Administration; 1997.

21. American Institute of Ultrasound in Medicine, National Electrical Manufacturers Association. Output Display Standard: Standard for Real-Time Display of Thermal and Mechanical Acoustic Output Indices on Diagnostic Ultrasound Equipment. Rev 1. Laurel, MD: American Institute of Ultrasound in Medicine; Rosslyn, VA: National Electrical Manufacturers Association; 1998.

22. Raum K, O'Brien WD Jr. Pulse-echo field distribution measurement technique of high-frequency ultrasound sources. IEEE Trans Ultrason Ferroelectr Freq Control 1997; 44:810–815.

23. American Institute of Ultrasound in Medicine, National Electrical Manufacturers Association. Acoustic Output Measurement Standard for Diagnostic Ultrasound Equipment. Laurel, MD: American Institute of Ultrasound in Medicine; Rosslyn, VA: National Electrical Manufacturers Association; 1998.

24. Teotico GA, Miller RJ, Frizzell LA, Zachary JF, O'Brien WD Jr. Attenuation coefficient estimates of mouse and rat chest wall. IEEE Trans Ultrason Ferroelectr Freq Control 2001; 48:593–601.

25. Towa RT, Miller RJ, Frizzell LA, Zachary JF, O'Brien WD Jr. Attenuation coefficient and propagation speed estimates of rat and pig intercostal tissue as a function of temperature. IEEE Trans Ultrason Ferroelectr Freq Control 2002; 49:1411–1420.

26. Sheehan DC, Hrapchak BB. Fixation. In: Theory and Practice of Histological Techniques. 2nd ed. St Louis, MO: CV Mosby Co; 1980:44–49.

27. Ihaka R, Gentleman R. R: a language for data analysis and graphics. J Comput Grap Stat 1996; 5:299–314.

28. Comprehensive R Archive Network. Available at: http://cran.r-project.org.

29. Hosmer DW, Lemeshow S. Applied Logistic Regression. 2nd ed. New York, NY: John Wiley & Sons; 2000.

30. Agresti A. An Introduction to Categorical Data Analysis. New York, NY: John Wiley & Sons; 1996.

31. Amemiya T. Tobit models: a survey. J Econ 1984; 24:3–61.

32. Galfalvy H, Simpson DG. Infrastructure degradation: an application of censored regression models. In: American Statistical Association Proceedings of the Section on Physical and Engineering Sciences, Alexandria, VA: American Statistical Association; 1999:242–247.

33. Raeman CH, Dalecki D, Child SZ, Meltzer RS, Carstensen EL. Albunex does not increase the sensitivity of the lung to pulsed ultrasound. Echocardiography 1997; 6:553–557.

34. Lerner RM, Carstensen EL, Dunn F. Frequency dependence of thresholds for ultrasonic production of thermal lesions in tissue. J Acoust Soc Am 1973; 54:504–506.